frontiers | Frontiers in Materials

TYPE Original Research
PUBLISHED 03 June 2024
DOI 10.3389/fmats.2024.1364828

OPEN ACCESS

EDITED BY
Mario Milazzo,
University of Pisa, Italy

REVIEWED BY
Danli Cui,
Chongqing Blood Center, China
Zetao Wang,
South China University of Technology, China

*CORRESPONDENCE
Hyoung-Taek Hong,
hyoungtaekhong@gmail.com
Kyoung-Tak Kang,
tagi1024@gmail.com

†These authors have contributed equally to this work

RECEIVED 15 February 2024
ACCEPTED 13 May 2024
PUBLISHED 03 June 2024

CITATION
Chang H-K, Koh Y-G, Hong H-T and Kang K-T (2024), Preparation of kartogenin-loaded PLGA microspheres and a study of their drug release profiles.
Front. Mater. 11:1364828.
doi: 10.3389/fmats.2024.1364828

Preparation of kartogenin-loaded PLGA microspheres and a study of their drug release profiles

Hyun-Kyung Chang[1], Yong-Gon Koh[2], Hyoung-Taek Hong[1*†] and Kyoung-Tak Kang[1,3*†]

[1]Skyve R&D LAB, Seoul, Republic of Korea, [2]Joint Reconstruction Center, Department of Orthopaedic Surgery, Yonsei Sarang Hospital, Seoul, Republic of Korea, [3]Department of Mechanical Engineering, Yonsei University, Seoul, Republic of Korea

Introduction: Kartogenin, a potent inducer of chondrogenic differentiation in mesenchymal stem cells and a key agent in cartilage regeneration, presents a viable therapeutic strategy for osteoarthritis management. Despite the abundance of literature on therapeutic potential of kartogenin, there is a paucity of studies characterizing the formulation specifics in microsphere fabrication. This exploration is pivotal to advances in regenerative medicine, particularly in the domain of cartilage regeneration, to assure clinical efficacy and safety.

Methods: In this work, we fabricated kartogenin-loaded PLGA microspheres with diverse formulations and their particle size, size distribution, encapsulation efficiency, drug loading and release profiles were characterized. Ratio of polymer, drug, and solvent and the use of surfactant was used as variables, and in particular, the effect of surfactant on particles was investigated.

Results: The average diameter of the spheres was 16.0–31.7 μm. Morphological variations from solid to porous surface structures depending on surfactant incorporation during the emulsification process was observed. Cumulative kartogenin release from microspheres ranged from 53.8% to 80.9% on day 28, and release profiles conform predominantly to the Korsmeyer-Peppas kinetics model.

Discussion: This study provides a foundational framework for modulating kartogenin release dynamics, a critical consideration for optimizing therapeutic efficacy and minimizing adverse effects in cartilage tissue engineering applications.

KEYWORDS

kartogenin, drug delivery system, PLGA microsphere, drug release profile, release kinetics

1 Introduction

Osteoarthritis is one of the most common degenerative joint disorders, affecting millions of people worldwide (Wieland et al., 2005). It occurs when the protective cartilage that protects the ends of bones wears away due to age, joint injury, or obesity (Lespasio et al., 2017). The main symptoms of osteoarthritis are joint pain, stiffness, and swelling, which can make it difficult to move (Sarzi-Puttini et al., 2005).

Cartilage, lacking blood vessels and nerves, is particularly prone to damage and challenging to repair (Wei et al., 2021). Current osteoarthritis treatments, including non-steroidal anti-inflammatory drugs and injections of viscoelastic hydrogels or steroids, offer only temporary pain relief and do not halt further joint damage (Sinusas, 2012).

Kartogenin (KGN), identified as a chondrogenic and chondroprotective agent, stimulates the differentiation of mesenchymal stem cells into chondrocytes, promoting cartilage repair (Kang et al., 2014; Ono et al., 2014). KGN binds filamin A, which disrupts its interaction with the transcription factor core-binding factor β subunit (CBFβ), and induces chondrogenesis by regulating the CBFβ-RUNX1 transcriptional program (Johnson et al., 2012). However, the therapeutic application of KGN is complicated by its potential to induce hyper-chondrogenesis at high doses (Zhang and Wang, 2014).

The clinical application of KGN is further challenged by its limited bioavailability and rapid degradation in physiological environments (Xu et al., 2021). To address these challenges, recent advancements have focused on drug delivery systems, including nano-encapsulation (Almeida et al., 2020; Fan et al., 2020), polymer-based scaffolds (Wang et al., 2019; Elder et al., 2022), and targeted delivery mechanisms (Jing et al., 2020), aiming to enhance stability of KGN, controlled release, and targeted delivery. Despite these advancements, there is still a significant gap in optimizing these delivery systems. One promising approach is the use of KGN-loaded microspheres made from biodegradable polymers such as PLGA, which could offer controlled and sustained release, improving therapeutic efficacy and minimizing side effects (Asgari et al., 2020; Zhao et al., 2020). PLGA has been widely used in tissue engineering due to its favorable biocompatibility and adjustable biodegradation (Gottardi et al., 2021; Zhou et al., 2022). With extensive research into the fabrication of these microspheres, it is crucial to understand the intricate balance of factors such as particle size, encapsulation efficiency, drug loading capacity, and release kinetics. These parameters directly impact the clinical efficacy and safety of the treatment, making their study essential in the advancement of regenerative medicine, especially for cartilage regeneration.

Our study provides a comprehensive characterization of formulation variables and their effects on the microspheres, laying the groundwork for optimizing KGN delivery. We hypothesized the following: (1) drug release profiles vary based on the drug-polymer to solvent ratio, and (2) the use of surfactants influences drug release profiles. This research is pivotal in advancing the field of cartilage tissue engineering, offering insights into developing more effective and safer therapeutic strategies for osteoarthritis and potentially other degenerative joint diseases.

2 Materials and methods

2.1 Materials

Poly (lactide-co-glycolic acid) with inherent viscosity 0.5–0.7 dL/g (PLGA, RESOMER RG 755 S) and poly (vinyl alcohol) (PVA, 87%–89% hydrolyzed, Mw = 13,000–23,000) were purchased from Sigma Aldrich Co. (USA). KGN was purchased from Combi-Blocks (USA). Dichloromethane (DCM), Tween 20, and Tween 80 were purchased from Duksan Pure Chemical Co. (Republic of Korea). Phosphate buffered saline (PBS) was purchased from Daejung Chemicals & Metals Co. (Republic of Korea). Dimethyl sulfoxide (DMSO) was purchased from Kanto Chemical Co. (Japan).

2.2 Preparation of KGN-loaded PLGA microspheres

PLGA microspheres were prepared using the oil-in-water (O/W) emulsion solvent evaporation method (Wischke and Schwendeman, 2008). Briefly, PLGA and KGN were dissolved in DCM and DMSO, respectively. The water phase consisted of 1% PVA as a stabilizer. Additionally, Tween 20, used as a surfactant, was added to the water phase at a final concentration of 0.05% according to the formulation listed in Table 1. The oil phase, composed of DCM and DMSO, was mixed and then added to 30 mL of water phase dropwise. Then, the O/W emulsion was magnetically mixed at 1,000 rpm and stirred overnight to evaporate the organic solvent. KGN-loaded microspheres were collected by centrifugation at 4,000 rpm for 10 min. The collected microspheres were washed with distilled water (DW) three times to remove PVA and DMSO residue and lyophilized at −60°C for 3 days. The samples were stored at −20°C until use. A graphical summary of the thesis is presented in Figure 1.

2.3 Characterization of KGN-loaded microspheres

The particle size of the microspheres was measured using a laser particle size analyzer with a Hydro 2000S accessory (Mastersizer 2000; Malvern). For this, 150 mg of each particle was dispersed in DW, and the measurement range was 0.02–2,000 μm. The span value representing the size distribution was calculated using the following equation:

$$Span = \frac{D90 - D10}{D50}$$

where D10, D50, and D90 are particle size at 10 vol%, 50 vol%, and 90 vol%, respectively.

Fourier transform infrared spectra (FTIR) of PLGA, KGN, and KGN-loaded microspheres were recorded in potassium bromide pellet using an FTIR spectrometer (VERTEX 80V, Bruker) to verify the chemical composition. Each sample was scanned 16 times in the range of 400–4,000 cm^{-1} at a resolution of 2 cm^{-1}.

The surface morphology of microspheres was characterized using a scanning electron microscope (SEM, Phenom XL, Thermo Fisher). The samples were coated with platinum (Pt) using an ion sputter coater, and images were obtained at a voltage of 15 kV.

To investigate the porosity of microspheres, focused ion beam SEM (FIB-SEM, Helios 5 UX, Thermo Fisher) was used for cross-sectional sample preparation and imaging of microspheres. Cross-section of microspheres was prepared by gallium ion beam, which can remove materials with a precision of a few nanometers with

TABLE 1 Parameters for preparation of formulation S1 to S8.

Formulation	PLGA (mg)	KGN (mg)	DCM (mL)	DMSO (mL)	Tween 20 (%)
S1	100	10	10	1	-
S2	100	10	10	1	0.05
S3	150	10	10	1	-
S4	150	10	10	1	0.05
S5	150	15	10	1	-
S6	150	15	10	1	0.05
S7	150	15	15	1	-
S8	150	15	15	1	0.05

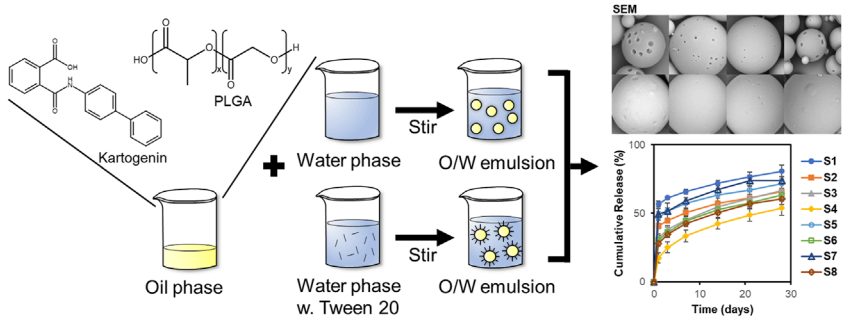

FIGURE 1
Graphical abstract of KGN-loaded PLGA microspheres preparation and characterization.

TABLE 2 Equation and parameters of release kinetic models including zero-order, first-order, Korsmeyer-Peppas, and Hixson-Crowell models.

Model	Equation	Parameters
Zero-order	$Q = Q_0 + K_0 t$	Q: the amount of drug released at time t Q_0: the initial amount of drug K: release constant n: release exponent
First-order	$Q = Q_0 e^{K_1 t}$	
Korsmeyer-Peppas	$Q = K_{KP} t^n$	
Hixson-Crowell	$Q^{1/3} = K_{HC} t + Q_0^{1/3}$	

negligible damage to the cross-section (Orloff et al., 2003). Cross-sectioning was carried at a 52-degree tilt angle and images of microspheres were obtained at a voltage of 2 kV using SEM.

Drug-loaded microspheres were dissolved in DMSO and diluted. The KGN content was determined by ultraviolet-visible (UV-vis) spectrometer (OPTIZEN POP, KLAB) and encapsulation efficiency (EE) and drug loading (DL) were calculated based on a standard curve. The EE and DL values were determined using the following equations:

$$EE(\%) = \frac{Amount\ of\ drug\ in\ Microspheres}{Amount\ of\ drug\ added} \times 100$$

$$DL(\%) = \frac{Amount\ of\ drug\ in\ Microspheres}{Amount\ of\ Microspheres} \times 100$$

2.4 *In vitro* KGN release study

In vitro drug release was tested using the centrifugation method (Kim et al., 2021). To measure the release profiles of KGN, 10 mg of each microsphere was dispersed in 10 mL of PBS (pH 7.4) containing 1% Tween 80. Tween 80 was used to ensure sink conditions for the released KGN (Gupta et al., 2022). The samples were gently agitated under 100 rpm in a shaking incubator (SHI1, LABTron) at 37°C. At a designated time, the supernatant was collected, and the same volume of fresh buffer was added to the sample tube before it was returned to the incubator. To assess the amount of KGN released, the maximum UV absorption wavelength of the KGN was measured at 282 nm using a UV-vis spectrometer. The KGN concentration was calculated based on a standard curve with the corresponding buffer solutions.

2.5 KGN release kinetics

The experimental KGN release profiles were evaluated depending on various mathematical models including zero-order, first-order, Korsmeyer-Peppas, and Hixson-Crowell models (Fu and Kao, 2010; Modi and Anderson, 2013). The equations and parameters of the release model are listed in Table 2. The KinetDS

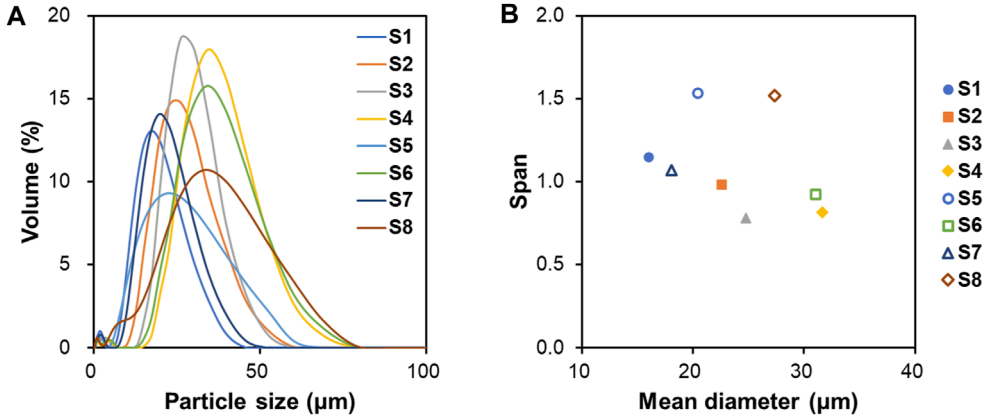

FIGURE 2
Particle characterization analyzed by laser particle size analyzer. **(A)** Particle size distribution, **(B)** Mean diameter and span value of S1 to S8.

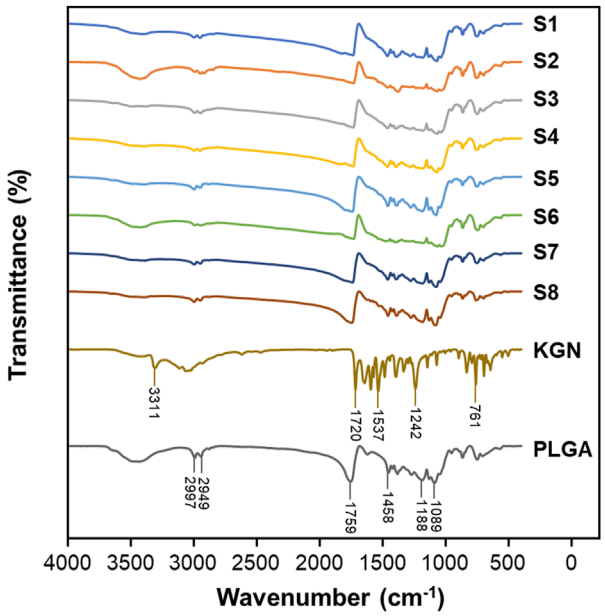

FIGURE 3
FTIR transmission spectra for S1, S2, S3, S4, S5, S6, S7, S8, KGN, and PLGA with in region 400–4,000 cm^{-1}.

software (version 3.0; Jagiellonian University Medical College, Krakow, Poland) was used to determine the release kinetics. The R^2 value was also calculated. The most appropriate fitted model was determined.

2.6 Statistical analysis

Data were presented as mean ± standard deviation from at least three replicates. The statistical differences between the two groups were determined by Student's t-test using SPSS software for Windows (version 12.0; SPSS, Chicago, IL, United States). Probability (p) values < 0.05 were considered statistically significant.

3 Results and discussion

3.1 Microsphere fabrication and morphological characterization

Microspheres were prepared through O/W emulsion using the solvent evaporation method. Eight samples (S1–S8) were dispersed in DW and then characterized by a wet method particle size analyzer (Figure 2). The size distribution of S1–S8 is shown in Figure 2A. The mean particle diameter increased in S2, S4, S6, and S8, which used Tween 20 as a surfactant compared to the non-surfactant conditions in S1, S3, S5, and S7. Surfactant has an overall effect on particle fabrication and causes an increase in particle size (Srinivasan and Shoyele, 2013). The microspheres had a mean particle size between 16.0 and 31.7 μm (Figure 2B). The span value, which indicates the width of particle size distribution, was in the range of 0.8–1.5. In particular, S3 and S4 had the lowest span value of 0.8, which indicates particles with uniform particle size and narrow size distribution among the samples.

FTIR spectra were used to confirm the chemical functional groups of the microspheres as shown in Figure 3. The characteristic peaks at 2,949 and 2,997 cm^{-1}, indicating the stretching of C-H, C-H_2 and C-H_3 functional groups of PLGA, were observed in the spectra of the microspheres. The peak of C=O stretching at 1759 cm^{-1} and the peak1 of C-O stretching at 1,089 cm^{-1} shifted to lower wavenumbers compared to the PLGA spectrum. As the shift of bands in the FTIR spectra is due to interactions between polymers and drugs by hydrogen bonds or electrostatic interactions (Fornaro et al., 2015), this change was attributed to the presence of KGN inside of the microspheres.

The morphology of the microspheres was analyzed by SEM (Figure 4). The particle distributions in Figures 4A–H are similar to the span values described in Figure 2. The surface morphology of the particles can be detected with high magnification, as in

10.3389/fmats.2024.1364828

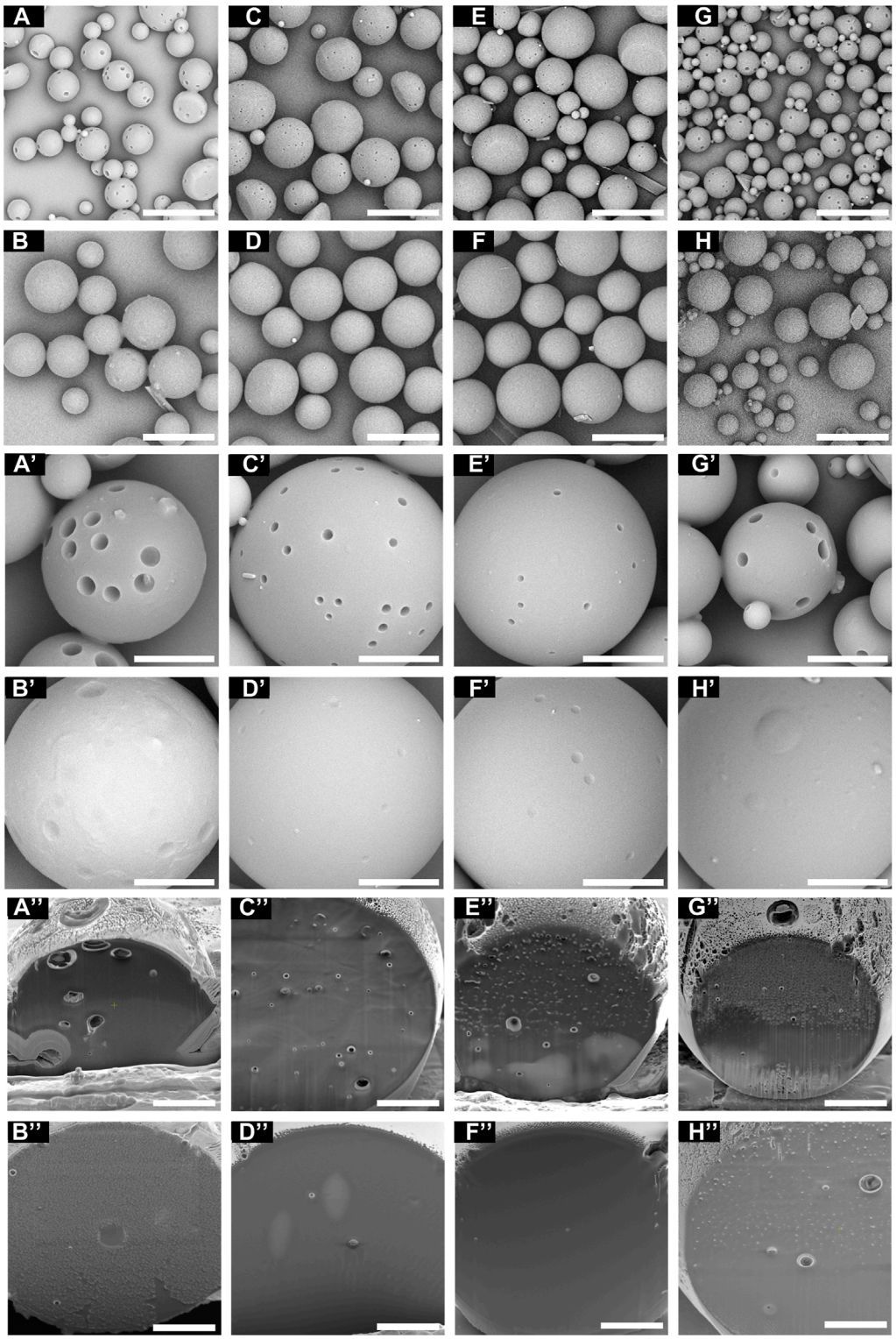

FIGURE 4
The surface of the microspheres under SEM at different magnifications. **(A)** S1, **(B)** S2, **(C)** S3, **(D)** S4, **(E)** S5, **(F)** S6, **(G)** S7, and **(H)** S8 (scale bar 40 μm). **(A′)** S1, **(B′)** S2, **(C′)** S3, **(D′)** S4, **(E′)** S5, **(F′)** S6, **(G′)** S7, and **(H′)** S8 (scale bar 10 μm). The cross-sectional images of the microspheres under FIB-SEM. **(A″)** S1, **(B″)** S2, **(C″)** S3, **(D″)** S4, **(E″)** S5, **(F″)** S6, **(G″)** S7, and **(H″)** S8 (scale bar 5 μm).

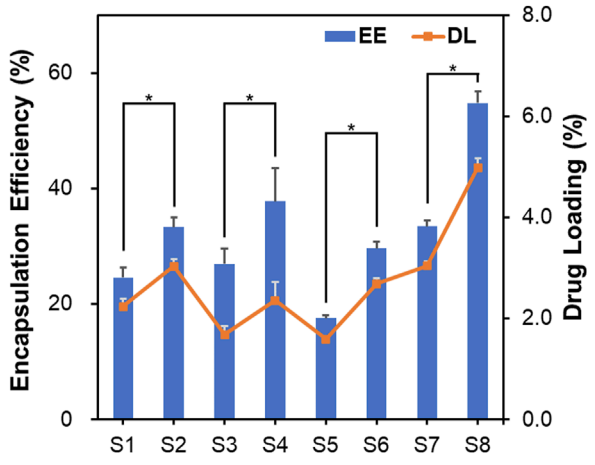

FIGURE 5
Encapsulation efficiency and drug loading capacity of microspheres. Data are presented as mean ± standard deviation (n = 3). * represents $p < 0.05$.

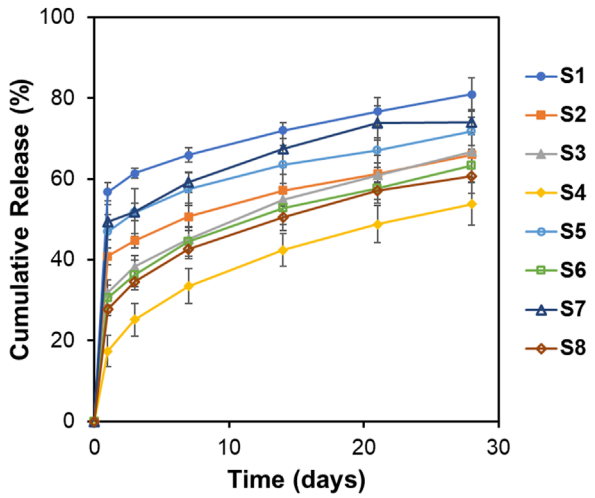

FIGURE 6
In vitro release profiles of KGN from PLGA microspheres in the PBS solution (pH = 7.4, 1% Tween 80) at 37°C for 28 days. Data are presented as mean ± standard deviation (n = 3).

Figures 4A'–H'. The type of surfactant added to the emulsion affects the surface morphology (Mohamed and van der Walle, 2006). S1, S3, S5, and S7 showed porous particle surfaces, with particularly large pore size in S1 and S7. Magnetic stirring at 1,000 rpm caused the DCM to evaporate rapidly and generated pores on the particle surface. Chung *et al.* reported that a fast solvent evaporation rate results in larger pores but smaller particle size (Chung et al., 2002). However, S2, S4, S6, and S8 had smooth particle surfaces without pores and larger particle size than the others. We suggest that it was the use of Tween 20 in the O/W emulsion that explains the creation of porous or non-porous surfaces. Tween 20 used in the preparation of S2, S4, S6, and S8 might slow the solvent evaporation rate, resulting in large, non-porous particles.

As FIB milling is one of the methods to cross-section the material without sample damage than mechanical cutting (Zhang et al., 2020), the cross-sectional images of microspheres were prepared and captured by the FIB-SEM (Figures 4A"–H"). S1 showed the largest pores on the cross-section of the microspheres, while S4 and S6 showed non-porous cross-section images. Microspheres with low porosity can be expected to have lower surface area and slow drug release and degradation rates.

3.2 Drug encapsulation

Several studies have reported that particle fabrication formulations, such as polymer concentration, solvent ratio, and surfactant, affect encapsulation efficiency of the drug-loaded particles (Lagreca et al., 2020; Sagoe et al., 2023). Figure 5 illustrates the encapsulation efficiency (EE) and drug loading capacity (DL) of the microspheres. While the p-value in Figure 5 indicates that the surfactant affects EE and DL significantly, there was no statistical significance between the DL of S3 and S5. This finding indicates that an increase in drug concentration does not affect the DL. However, EE decreases when the drug concentration increases. The organic solvent ratio affects both EE and DL. In particular, S8 showed a high performance with an EE of 54.8% and DL of 5.0% among the samples.

Additionally, we suggest that the organic solvent affects the drug-loading characteristics. In this study, the organic solvent used in the O/W emulsion was evaporated with overnight stirring. However, the DMSO used to dissolve KGN does not evaporate easily due to its high boiling point of 189°C. In contrast, DCM evaporates easily at a low temperature. The relatively low EE of KGN might be attributed to its high solubility in DMSO. Its EE value might be complemented by the use of Tween 20, because surfactant with HLB values >15 has been shown to increase the EE of hydrophobic drugs in PLGA microspheres (Dinarvand et al., 2005).

3.3 Drug release study

3.3.1 Release profile

The release of KGN from the microspheres was monitored for 28 days (Figure 6). Tween 80 was used to ensure the sink conditions in the release test. An initial burst drug release (56.8, 40.9, 31.9, 17.4, 47.0, 30.5, 49.3, and 27.9%) was observed on day 1, which might be due to diffusion of the drug on the surface of the particles into the solution (Allison, 2008; Yoo and Won, 2020). In particular, the cumulative release of S1 and S7 reached approximately 70% on day 14. Also, as both polymer and drug are hydrophobic, the ratio of polymer to drug is important. Among the samples, S4, a formulation with surfactant and a high PLGA content, demonstrated the lowest initial burst and released KGN constantly. The drug polymer ratio affects drug release; the release profiles could be slowed as polymer amount increases (Kilicarslan and Baykara, 2003). On day 28, the cumulative drug release percentages were 80.9, 66.0, 66.7, 53.8, 71.8, 63.3, 74.0, and 60.7%, respectively. These results revealed drug release for 4 weeks and suggested that the microspheres are suitable for long-term treatment.

TABLE 3 Release constant (K) and regression coefficient (R^2) for each kinetic model and diffusion exponent (n) for the Korsmeyer-Peppas model.

	Zero-order		First-order		Korsmeyer-peppas			Hixson-crowell	
	K_0	R^2	K_1	R^2	K_{KP}	R^2	n	K_{HC}	R^2
S1	0.8529	0.9686	0.0124	0.9494	55.442	0.9693	0.1047	0.0169	0.9563
S2	0.8989	0.9644	0.0169	0.9375	39.423	0.9730	0.1443	0.0212	0.9473
S3	1.2437	0.9626	0.0256	0.9171	30.733	0.9860	0.2233	0.0310	0.9342
S4	1.2771	0.9406	0.0372	0.8499	17.378	0.9999	0.3384	0.0400	0.8846
S5	0.8631	0.9497	0.0145	0.9219	45.922	0.9834	0.1258	0.0189	0.9318
S6	1.1586	0.9475	0.0251	0.8970	29.503	0.9910	0.2209	0.0299	0.9156
S7	0.9763	0.9256	0.0158	0.9072	47.064	0.9509	0.1353	0.0208	0.9134
S8	1.1701	0.9375	0.0266	0.8801	27.279	0.9963	0.2373	0.0312	0.9013

Particle size and surface morphology affect the drug release profiles. Kilicarslan *et al.* reported that particles with high porosity have a faster drug release rate than do particles with low porosity (Schnieders et al., 2011). As shown in Figure 6, formulations with large particle size (S4, S6, and S8) had relatively slower drug release than did formulations with small particle size (S1, S7, and S5). With regard to surface morphology, S1 and S7 demonstrated fast drug release because of the large surface pores that are observed on SEM images. In contrast, drug release was slower with non-porous particles. These findings suggest that characterization of microspheres, particle size analysis, and SEM are important in drug release.

The drug release profiles of microspheres significantly impact the treatment of osteoarthritis by affecting the duration and efficacy. Firstly, a stable and controlled release rate ensures a steady supply of the therapeutic agent over an extended period. The controlled release rate minimizes the risk of local and systemic side effects and reduces the potential for toxicity while maintaining effective therapeutic levels. This is especially important in the treatment of osteoarthritis, where long-term drug use is common. Secondly, the use of formulations that provide controlled release may reduce the need for frequent dosing, which improves the quality of life of patients. Additionally, reducing the frequency of dosing and improving disease management may lower the overall healthcare costs associated with treating osteoarthritis. In this regard, the drug release rate from PLGA microspheres plays a pivotal role in determining the effectiveness, safety, and convenience of treatments. Optimizing the release rate is crucial for achieving the best therapeutic outcomes, minimizing side effects, and improving patient compliance and quality of life.

3.3.2 Release kinetics

The release kinetics are determined based on cumulative release data using the following four kinetic models; zero-order, first-order, Korsmeyer-Peppas, and Hixson-Crowell models (Dash et al., 2010). To investigate the suitable drug release kinetic model, the regression coefficient value (R^2) was calculated, and the model with R^2 closest to 1 is the best fit (Table 3). The release data were applied from days 1–28. The Korsmeyer-Peppas model was the best fit to KGN release kinetics of the PLGA microspheres. Moreover, the release kinetics of S4 showed the best fit with the Korsmeyer-Peppas model, with an R^2 Value of 0.9999. The diffusion exponent (n) represents the diffusion mechanism in the Korsmeyer-Peppas model. An n value <0.5 indicates Fickian diffusion, which occurs by the usual molecular diffusion of the drug due to a chemical potential gradient.

3.4 Expectations and limitations

KGN-loaded PLGA microspheres could potentially contribute to the treatment of osteoarthritis using intra-articular injection drug delivery system. PLGA microspheres were fabricated under various conditions and optimized with stable drug release for 1 month. It ensures a stable therapeutic concentration directly at the defect over prolonged periods, eliminating the need for frequent injections. Also, by adjusting the formulation of PLGA microspheres, it is possible to tailor the release profile of KGN by adjusting factors such as polymer to drug ratio, usage of surfactant, and particle size of the microspheres. This has the potential to optimize the therapeutic efficacy and improve the quality of life for patients suffering from osteoarthritis.

However, there are two major limitations in this study. The first is that the intra-articular environment, including drug clearance rate, presence of various enzymes, and mechanical stress within the joint, was not applied in the *in vitro* release test, and the degradation rate of PLGA was not investigated. Microspheres in the presence of various enzymes and mechanical stresses can be characterized differently from the typical *in vitro* environment. As the above tests are difficult to mimic the intra-articular environment in an *in vitro* test, further *in vivo* experiments are needed to determine the drug release and degradation of the microspheres in intra-articular injection drug delivery systems. The second limitation is that we were not able to confirm the effectiveness of the KGN-loaded microspheres for osteoarthritis. Although KGN is known to

promote chondrogenic differentiation, it remains to be determined whether PLGA microspheres are synergistic agents for the treatment of osteoarthritis. PLGA microspheres have been widely used for controlled-release drug delivery. However, there is a lack of papers investigating the influence of surfactant tween-80 and comparing the KGN release profiles of different formulations. Despite the limitations, these findings could be the basis for KGN delivery using PLGA microspheres for intra-articular injection.

4 Conclusion

In summary, we successfully developed PLGA microspheres for the effective delivery of KGN. Our findings revealed that factors such as the usage of surfactant, and the ratios of polymer to solvent, significantly influence the microspheres' properties, ranging from particle size to drug release behavior. Notably, *in vitro* experiments showed that these KGN-loaded microspheres could achieve sustained release over nearly a month, aligning with the requirements for long-term release formulations. Among the various formulations tested, S4 emerged as the most promising, exhibiting an optimal drug release profile that conformed to the Korsmeyer-Peppas model. However, further *in vitro* and *in vivo* studies are necessary to fully understand the therapeutic potential of these KGN-loaded microspheres. Overall, our results suggest that this KGN-loaded microsphere system holds great promise for applications in cartilage tissue engineering.

Data availability statement

The original contributions presented in the study are included in the article/Supplementary material, further inquiries can be directed to the corresponding authors.

Author contributions

H-KC: Writing–original draft, Visualization, Formal Analysis, Data curation, Conceptualization. Y-GK: Writing–review and editing, Supervision, Resources, Methodology. H-TH: Writing–review and editing, Project administration, Data curation, Conceptualization. K-TK: Writing–review and editing, Supervision, Project administration, Conceptualization.

Funding

The author(s) declare that no financial support was received for the research, authorship, and/or publication of this article.

Conflict of interest

Authors H-KC, H-TH and K-TK were employed by company Skyve.

The remaining author declares that the research was conducted in the absence of any commercial or financial relationships that could be construed as a potential conflict of interest.

Publisher's note

References

Allison, S. D. (2008). Analysis of initial burst in PLGA microparticles. *Expert Opin. Drug Deliv.* 5 (6), 615–628. doi:10.1517/17425247.5.6.615

Almeida, B., Wang, Y., and Shukla, A. (2020). Effects of nanoparticle properties on kartogenin delivery and interactions with mesenchymal stem cells. *Ann. Biomed. Eng.* 48 (7), 2090–2102. doi:10.1007/s10439-019-02430-x

Asgari, N., Bagheri, F., Eslaminejad, M. B., Ghanian, M. H., Sayahpour, F. A., and Ghafari, A. M. (2020). Dual functional construct containing kartogenin releasing microtissues and curcumin for cartilage regeneration. *Stem Cell Res. Ther.* 11 (1), 289. doi:10.1186/s13287-020-01797-2

Chung, T. W., Huang, Y. Y., Tsai, Y. L., and Liu, Y. Z. (2002). Effects of solvent evaporation rate on the properties of protein-loaded PLLA and PDLLA microspheres fabricated by emulsion-solvent evaporation process. *J. Microencapsul.* 19 (4), 463–471. doi:10.1080/02652040210140706

Dash, S., Murthy, P. N., Nath, L., and Chowdhury, P. (2010). Kinetic modeling on drug release from controlled drug delivery systems. *Acta Pol. Pharm.* 67 (3), 217–223.

Dinarvand, R., Moghadam, S. H., Sheikhi, A., and Atyabi, F. (2005). Effect of surfactant HLB and different formulation variables on the properties of poly-D,L-lactide microspheres of naltrexone prepared by double emulsion technique. *J. Microencapsul.* 22 (2), 139–151. doi:10.1080/02652040400026392

Elder, S., Roberson, J. G., Warren, J., Lawson, R., Young, D., Stokes, S., et al. (2022). Evaluation of electrospun PCL-PLGA for sustained delivery of kartogenin. *Molecules* 27 (12), 3739. doi:10.3390/molecules27123739

Fan, W., Yuan, L., Li, J., Wang, Z., Chen, J., Guo, C., et al. (2020). Injectable double-crosslinked hydrogels with kartogenin-conjugated polyurethane nano-particles and transforming growth factor β3 for *in-situ* cartilage regeneration. *Mater Sci. Eng. C Mater Biol. Appl.* 110, 110705. doi:10.1016/j.msec.2020.110705

Fornaro, T., Burini, D., Biczysko, M., and Barone, V. (2015). Hydrogen-bonding effects on infrared spectra from anharmonic computations: uracil-water complexes and uracil dimers. *J. Phys. Chem. A* 119 (18), 4224–4236. doi:10.1021/acs.jpca.5b01561

Fu, Y., and Kao, W. J. (2010). Drug release kinetics and transport mechanisms of non-degradable and degradable polymeric delivery systems. *Expert Opin. Drug Deliv.* 7 (4), 429–444. doi:10.1517/17425241003602259

Gottardi, R., Moeller, K., Di Gesù, R., Tuan, R. S., van Griensven, M., and Balmayor, E. R. (2021). Application of a hyperelastic 3D printed scaffold for mesenchymal stem cell-based fabrication of a bizonal tendon enthesis-like construct. *Front. Mater.* 8. doi:10.3389/fmats.2021.613212

Gupta, R., Chen, Y., Sarkar, M., and Xie, H. (2022). Surfactant mediated accelerated and discriminatory *in vitro* drug release method for PLGA nanoparticles of poorly water-soluble drug. *Pharm. (Basel)* 15 (12), 1489. doi:10.3390/ph15121489

Jing, H., Zhang, X., Luo, K., Luo, Q., Yin, M., Wang, W., et al. (2020). miR-381-abundant small extracellular vesicles derived from kartogenin-preconditioned mesenchymal stem cells promote chondrogenesis of MSCs by targeting TAOK1. *Biomaterials* 231, 119682. doi:10.1016/j.biomaterials.2019.119682

Johnson, K., Zhu, S., Tremblay, M. S., Payette, J. N., Wang, J., Bouchez, L. C., et al. (2012). A stem cell-based approach to cartilage repair. *Science* 336 (6082), 717–721. doi:10.1126/science.1215157

Kang, M. L., Ko, J. Y., Kim, J. E., and Im, G. I. (2014). Intra-articular delivery of kartogenin-conjugated chitosan nano/microparticles for cartilage regeneration. *Biomaterials* 35 (37), 9984–9994. doi:10.1016/j.biomaterials.2014.08.042

Kilicarslan, M., and Baykara, T. (2003). The effect of the drug/polymer ratio on the properties of the verapamil HCl loaded microspheres. *Int. J. Pharm.* 252 (1-2), 99–109. doi:10.1016/s0378-5173(02)00630-0

Kim, Y., Park, E. J., Kim, T. W., and Na, D. H. (2021). Recent progress in drug release testing methods of biopolymeric particulate system. *Pharmaceutics* 13 (8), 1313. doi:10.3390/pharmaceutics13081313

Lagreca, E., Onesto, V., Di Natale, C., La Manna, S., Netti, P. A., and Vecchione, R. (2020). Recent advances in the formulation of PLGA microparticles for controlled drug delivery. *Prog. Biomater.* 9 (4), 153–174. doi:10.1007/s40204-020-00139-y

Lespasio, M. J., Piuzzi, N. S., Husni, M. E., Muschler, G. F., Guarino, A., and Mont, M. A. (2017). Knee osteoarthritis: a primer. *Perm. J.* 21, 16–183. doi:10.7812/TPP/16-183

Modi, S., and Anderson, B. D. (2013). Determination of drug release kinetics from nanoparticles: overcoming pitfalls of the dynamic dialysis method. *Mol. Pharm.* 10 (8), 3076–3089. doi:10.1021/mp400154a

Mohamed, F., and van der Walle, C. F. (2006). PLGA microcapsules with novel dimpled surfaces for pulmonary delivery of DNA. *Int. J. Pharm.* 311 (1-2), 97–107. doi:10.1016/j.ijpharm.2005.12.016

Ono, Y., Ishizuka, S., Knudson, C. B., and Knudson, W. (2014). Chondroprotective effect of kartogenin on CD44-mediated functions in articular cartilage and chondrocytes. *Cartilage* 5 (3), 172–180. doi:10.1177/1947603514528354

Orloff, J., Swanson, L., and Utlaut, M. W. (2003). *High resolution focused ion beams: FIB and its applications: the physics of liquid metal ion sources and ion optics and their application to focused ion beam technology*. New York: Kluwer Academic/Plenum Publishers.

Sagoe, P. N. K., Velazquez, E. J. M., Espiritusanto, Y. M., Gilbert, A., Orado, T., Wang, Q., et al. (2023). Fabrication of PEG-PLGA microparticles with tunable sizes for controlled drug release application. *Molecules* 28 (18), 6679. doi:10.3390/molecules28186679

Sarzi-Puttini, P., Cimmino, M. A., Scarpa, R., Caporali, R., Parazzini, F., Zaninelli, A., et al. (2005). Osteoarthritis: an overview of the disease and its treatment strategies. *Semin. Arthritis Rheum.* 35 (1), 1–10. doi:10.1016/j.semarthrit.2005.01.013

Schnieders, J., Gbureck, U., Vorndran, E., Schossig, M., and Kissel, T. (2011). The effect of porosity on drug release kinetics from vancomycin microsphere/calcium phosphate cement composites. *J. Biomed. Mater Res. B Appl. Biomater.* 99 (2), 391–398. doi:10.1002/jbm.b.31910

Sinusas, K. (2012). Osteoarthritis: diagnosis and treatment. *Am. Fam. Physician* 85 (1), 49–56.

Srinivasan, A. R., and Shoyele, S. A. (2013). Self-associated submicron IgG1 particles for pulmonary delivery: effects of non-ionic surfactants on size, shape, stability, and aerosol performance. *AAPS PharmSciTech* 14 (1), 200–210. doi:10.1208/s12249-012-9913-1

Wang, S. J., Qin, J. Z., Zhang, T. E., and Xia, C. (2019). Intra-articular injection of kartogenin-incorporated thermogel enhancing osteoarthritis treatment. *Front. Chem.* 7, 677. doi:10.3389/fchem.2019.00677

Wei, W., Ma, Y., Yao, X., Zhou, W., Wang, X., Li, C., et al. (2021). Advanced hydrogels for the repair of cartilage defects and regeneration. *Bioact. Mater* 6 (4), 998–1011. doi:10.1016/j.bioactmat.2020.09.030

Wieland, H. A., Michaelis, M., Kirschbaum, B. J., and Rudolphi, K. A. (2005). Osteoarthritis - an untreatable disease? *Nat. Rev. Drug Discov.* 4 (4), 331–344. doi:10.1038/nrd1693

Wischke, C., and Schwendeman, S. P. (2008). Principles of encapsulating hydrophobic drugs in PLA/PLGA microparticles. *Int. J. Pharm.* 364 (2), 298–327. doi:10.1016/j.ijpharm.2008.04.042

Xu, X., Liang, Y., Li, X., Ouyang, K., Wang, M., Cao, T., et al. (2021). Exosome-mediated delivery of kartogenin for chondrogenesis of synovial fluid-derived mesenchymal stem cells and cartilage regeneration. *Biomaterials* 269, 120539. doi:10.1016/j.biomaterials.2020.120539

Yoo, J., and Won, Y. Y. (2020). Phenomenology of the initial burst release of drugs from PLGA microparticles. *ACS Biomater. Sci. Eng.* 6 (11), 6053–6062. doi:10.1021/acsbiomaterials.0c01228

Zhang, J., and Wang, J. H. (2014). Kartogenin induces cartilage-like tissue formation in tendon-bone junction. *Bone Res.* 2, 14008. doi:10.1038/boneres.2014.8

Zhang, S., Wu, D., and Zhou, L. (2020). Characterization of controlled release microspheres using FIB-SEM and image-based release prediction. *AAPS PharmSciTech* 21 (5), 194. doi:10.1208/s12249-020-01741-w

Zhao, Y., Zhao, X., Zhang, R., Huang, Y., Li, Y., Shan, M., et al. (2020). Cartilage extracellular matrix scaffold with kartogenin-encapsulated PLGA microspheres for cartilage regeneration. *Front. Bioeng. Biotechnol.* 8, 600103. doi:10.3389/fbioe.2020.600103

Zhou, C., Su, S., Fan, J., Lin, J., and Wang, X. (2022). Engineered electrospun poly(lactic-co-glycolic acid)/Si3N4 nanofiber scaffold promotes osteogenesis of mesenchymal stem cell. *Front. Mater.* 9. doi:10.3389/fmats.2022.991018